

# EARTH, INTERIOR STRUCTURE OF THE

SHUN-ICHIRO KARATO, *Department of Geology and Geophysics, University of Minnesota, Minneapolis, Minnesota, U.S.A.*

EIJI OHTANI, *Institute of Mineralogy, Petrology and Economic Geology, Tohoku University, Sendai, Japan*

	<b>Introduction</b> . . . . .	1	3.1	Melting and Chemical Stratification . . . . .	14
<b>1.</b>	<b>Earth's Gross Structure</b> . . . . .	2	3.2	Magmatism and Melting of the Earth's Interior . . . . .	14
1.1	Geophysical and Geochemical Observations . . . . .	2	3.2.1	Mafic Magmas . . . . .	14
1.1.1	Seismology and the Earth's Interior . . . . .	2	3.2.2	Silicic and Intermediate Magmas . . . . .	14
1.1.2	Solar Abundance and the Bulk Composition of Silicate Earth . . . . .	5	3.2.3	Ultramafic Magmas and Melting in the Deep Mantle . . .	14
1.2	The Composition of the Earth . . . . .	6	<b>4.</b>	<b>Earth's Rheological Structure and Dynamics of the Earth's Interior</b> . . . . .	15
1.2.1	The Crust . . . . .	6	4.1	Time-Dependent Deformation of the Earth . . . . .	15
1.2.2	The Mantle . . . . .	6	4.2	Earth's Rheological Stratification . . . . .	17
1.2.2.1	The Upper Mantle . . . . .	6	4.3	Dynamics of the Earth's Interior . . . . .	18
1.2.2.2	The Transition Zone . . . . .	7	4.3.1	Plate Tectonics . . . . .	18
1.2.2.3	The Lower Mantle . . . . .	9	4.3.2	Seismic Tomography and Deep-Mantle Dynamics . . . . .	18
1.2.2.4	The <i>D''</i> Layer and the Core-Mantle Boundary . . . . .	9	4.3.3	Geochemical Observations on Mantle Heterogeneities . . . . .	19
1.2.3	The Core . . . . .	9	<b>5.</b>	<b>Summary</b> . . . . .	20
<b>2.</b>	<b>Earth's Thermal Regimes</b> . . . . .	10		<b>Glossary</b> . . . . .	20
2.1	Introduction . . . . .	10		<b>Works Cited</b> . . . . .	20
2.2	Heat Flow and Near-Surface Temperature Profile . . . . .	11		<b>Further Reading</b> . . . . .	20
2.3	Temperature Profiles of the Earth's Deep Interior . . . . .	11			
2.4	Thermal History . . . . .	13			
<b>3.</b>	<b>Melting of Silicates and Magmatism</b> . . . . .	14			

## INTRODUCTION

The Earth's deep interior is largely inaccessible (the deepest hole at Kola peninsula in Russia is ~12 km, only ~0.2% of the Earth's radius), and consequently most of our understanding is based on indirect inferences. These include the average chemical composition of the solar system, the chemical composition of rocks near the Earth's surface, geophysical observations of the Earth's density and of seismic wave-velocity distribution, and labo-

ratory studies of the state and properties of materials at high pressures and temperatures. Recent progress has also been made to increase the resolution in inversion of the Earth's structure through seismic tomography and developments in high-pressure and high-temperature experimental studies.

Section 1 of this article discusses the gross Earth structure, i.e., the major constituent materials of the crust, mantle, and core. Section 2 discusses the Earth's temperature distribution, which is determined by the heat

generation and heat transfer processes. The temperature distribution determines the Earth's rheological stratification and has a significant effect on dynamics (see Sec. 4). Section 3 summarizes experimental observations on the melting of silicates. Finally, Sec. 4 gives a brief summary of rheological properties of rocks and the dynamics of the Earth's interior.

## 1. EARTH'S GROSS STRUCTURE

### 1.1 Geophysical and Geochemical Observations

**1.1.1 Seismology and the Earth's Interior (see also SEISMOLOGY).** Table 1 summarizes some of the important parameters of the Earth. Note that the Earth's average density,  $5.52 \times 10^3 \text{ kg/m}^3$ , is significantly higher than the densities of rocks found on the Earth's surface [ $(2.7\text{--}3.4) \times 10^3 \text{ kg/m}^3$ ]. Another observation is that the ratio  $C/MR^2 = 0.331$  ( $C$ , moment of inertia;  $M$ , mass;  $R$ , radius) is significantly smaller than the theoretical value for a homogeneous body (0.40). These observations show that the density of the Earth must increase significantly with depth. This density increase is due to two factors: the existence of a dense iron-rich core and the increase in density due to hydrostatic compression within the Earth.

The most detailed information on the variation of physical properties or composition of the Earth with depth comes from seismological observations of elastic-wave propagation in the Earth. Various types of elastic waves are used to probe the Earth, including body waves, surface waves, and the free oscillation of the Earth.

The vibrations of the Earth due to natural earthquakes or artificial explosions are recorded on seismograms. Seismic waves recorded at a long distance from the focal point of an earthquake pass through deeper por-

tions of the Earth's interior than waves recorded at a nearby station. Similarly, the surface waves and the free oscillation of the Earth with a longer period reflect the properties of deeper portions of the Earth than those with a shorter period. Thus using the seismograms at different stations, or the surface-wave or free-oscillation records with different periods, one can estimate the depth variation of elastic properties and density. The information used includes the travel times of body waves, the frequency dependence of surface-wave velocities, and the frequencies of various modes of free oscillation.

In an isotropic elastic body, there are two different modes of elastic waves: compressional and shear waves. The velocities of these waves ( $V_p$ , velocity of compressional wave;  $V_s$ , velocity of shear wave) are related to the physical properties by

$$V_p = \sqrt{(K + \frac{4}{3}\mu)/\rho} \quad (1)$$

and

$$V_s = \sqrt{\mu/\rho}, \quad (2)$$

respectively, where  $K$  is incompressibility,  $\mu$  is rigidity, and  $\rho$  is density. These relations are exact only for an isotropic material, but will be sufficient for the purpose of the present section. However, when the fine details of seismic wave propagation are used to discuss the dynamics of the Earth's interior, the consideration of anisotropy becomes important (see Sec. 4.3.2).

An Earth model (depth variation of seismic wave velocities and densities) based on seismological data is shown in Fig. 1. This model (called PREM, for preliminary reference earth model; see Anderson, 1989) incorporates such details as the frequency dependence of seismic-wave velocities and attenuation but neglects the lateral variation and the azimuthal anisotropy (variation of seismic-wave velocities with the orientation of wave propagation; see Sec. 4.3.2). The gross Earth structure discussed in Sec. 1 is mainly based on the laterally averaged model (except for the crust).

Such an Earth model indicates that the Earth's interior is divided into three layers; the crust, the mantle, and the core. Once an Earth model is obtained, one can infer the internal constitution of the Earth by comparing the model with laboratory data on density

**Table 1.** Earth parameters.

Total mass, $M$	$5.97 \times 10^{24} \text{ kg}$
Mean radius, $R$	6371 km
Mean density, $\rho$	$5.52 \times 10^3 \text{ kg/m}^3$
Moment of inertia, $C^a$	$8.04 \times 10^{37} \text{ kg m}^2$
$C/MR^2$	0.331

<sup>a</sup>  $C = (8\pi/3) \int_0^R \rho(r) r^4 dr$

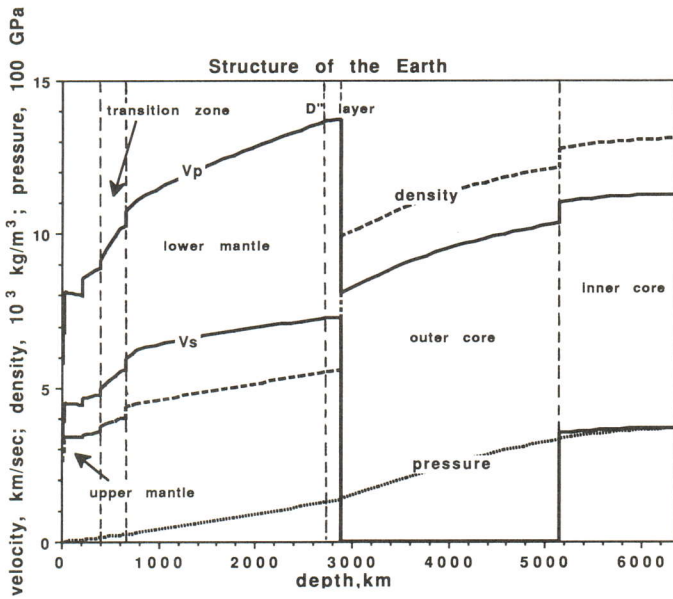


FIG. 1. The depth variation of the average seismic-wave velocities, densities, and pressure according to the PREM model.

and elastic properties with the help of physics of materials under high pressures and temperatures. Such studies indicate that these three layers have quite different chemical composition: The crust is mainly composed of silica-rich minerals such as quartz ( $\text{SiO}_2$ ) and feldspars [ $\text{CaAl}_2\text{Si}_2\text{O}_8$ ,  $(\text{K},\text{Na})\text{AlSi}_3\text{O}_8$ ], while the mantle is composed of magnesium- and iron-rich minerals such as olivine [ $(\text{Mg},\text{Fe})_2\text{SiO}_4$ ] and pyroxenes [ $(\text{Mg},\text{Fe},\text{Ca})\text{SiO}_3$ ] and their high-pressure polymorphs. The core is composed mainly of iron and some other alloying elements. The details of compositions of each layer will be discussed in Sec. 1.2.

The Earth structure thus inferred may be compared with a theoretical prediction of depth variation of density and of seismic-wave velocities for an ideal situation, that is,

the depth variation of these properties in an adiabatically compressed homogeneous body (a situation corresponding to a vigorously convecting layer without phase transformations). The density change in a homogeneous body due to adiabatic compression is given by

$$\frac{d\rho(r)}{dr} = \left(\frac{\partial\rho}{\partial P}\right)_S \frac{dP(r)}{dr}, \quad (3)$$

where  $r$  is the distance from the center of the Earth,  $(\partial\rho/\partial P)_S$  indicates the pressure dependence of density at adiabatic conditions, and  $P$  is the pressure. Now, as we shall see (Secs. 2 and 4), the temperature in the Earth is high enough to make rocks soft, and therefore no significant nonhydrostatic stresses can be maintained over geological time scales. Thus

**Table 2.** Density and elastic properties of typical minerals (at room temperature and room pressure).

Mineral	Density, $\rho$ ( $10^3 \text{ kg/m}^3$ )	Incompressibility, $K$ (GPa)	Rigidity, $\mu$ (GPa)
Quartz, $\text{SiO}_2$	2.65	38	44
Feldspar (anorthite), $\text{CaAl}_2\text{Si}_2\text{O}_8$	2.76	90	40
Olivine, $\text{Mg}_2\text{SiO}_4$	3.22	129	82
Modified spinel, $\text{Mg}_2\text{SiO}_4$	3.47	174	114
Spinel, $\text{Mg}_2\text{SiO}_4$	3.55	184	119
Pyroxene (enstatite), $\text{MgSiO}_3$	3.20	104	77
Garnet (majorite), $\text{MgSiO}_3$	3.52	175	90
Perovskite, $\text{MgSiO}_3$	4.10	246	184
Magnesiowüstite, $\text{MgO}$	3.58	163	131
Iron, Fe	7.87	172	83

the hydrostatic equilibrium is a very good approximation. Hence, we get

$$\frac{dP(r)}{dr} = -g(r)\rho(r) = -\frac{GM(r)\rho(r)}{r^2}, \quad (4)$$

where  $g(r)$  is the gravitational acceleration at  $r$ ,  $G$  is the gravitation constant, and  $M(r)$  is the mass of a sphere within the radius  $r$ , which is given by

$$M(r) = 4\pi \int_0^r \xi^2 \rho(\xi) d\xi. \quad (5)$$

The change in density with pressure is given by the incompressibility  $K(r)$  which is related to the observed seismic-wave velocities through

$$\begin{aligned} K(r) &= \rho(r) \left( \frac{\partial P}{\partial \rho} \right)_S \\ &= \rho(r) \left( V_p^2(r) - \frac{4}{3} V_s^2(r) \right) \\ &= \rho(r) \Phi(r), \end{aligned} \quad (6)$$

where  $\Phi(r)$  is the seismic parameter defined by  $\Phi = V_p^2 - \frac{4}{3} V_s^2$ . Combining Eqs. (3)–(6) one gets the Adams–Williamson equation that describes the depth variation of density due to adiabatic compression of a homogeneous body,

$$\frac{d\rho(r)}{dr} = -\frac{\rho(r)g(r)}{\Phi(r)} = -\frac{4\pi G\rho(r)}{\Phi(r)r^2} \int_0^r \xi^2 \rho(\xi) d\xi. \quad (7)$$

The pressure in the Earth can also be calculated from the estimated densities using Eq. (4).

A useful application of the Adams–Williamson equation is to examine how the real Earth structure is different from the idealized state of adiabatic compression of a homogeneous body. This can be done by calculating the inhomogeneity parameter, defined as

$$\eta_B(r) = -\frac{d\rho(r)}{dr} \frac{\Phi(r)}{\rho(r)g(r)}, \quad (8)$$

from the inferred density and seismic-wave velocity distributions. For a homogeneous body compressed adiabatically,  $\eta_B = 1$ . Here  $\eta_B > 1$  implies that the density increases with depth more than in an adiabatically compressed homogeneous body. A typical example includes the density increase due to phase transformations. In contrast,  $\eta_B < 1$  implies that density does not increase with depth as much as in an adiabatically compressed homogeneous body. A typical example is the case where the temperature gradient is higher than the adiabatic gradient. Changes in chemical composition with depth can also cause the deviation of  $\eta_B$  from 1. Figure 2 shows the inhomogeneity parameter in the Earth. It is seen that the core and the lower mantle are very close to an adiabatically compressed homogeneous body, but significant deviations are observed in the shallow upper mantle

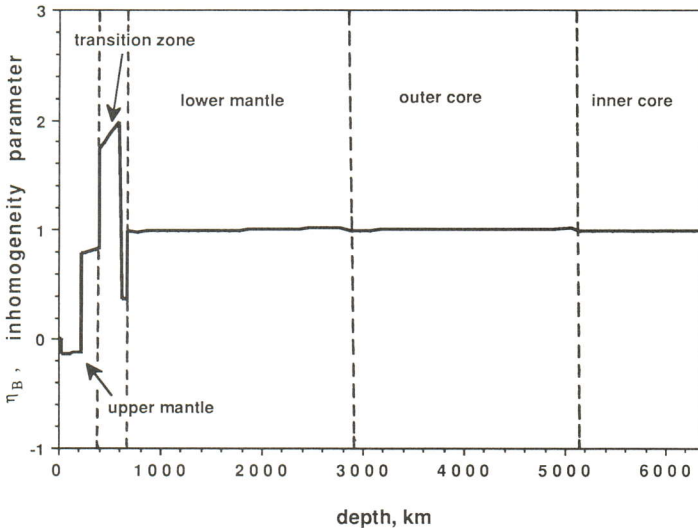


FIG. 2. The depth variation of the inhomogeneity parameter. The deviation from homogeneity ( $\eta_B = 1$ ) is significant in the upper mantle and in the transition zone.

(down to ~200 km) and in the transition zone (400–670 km). We shall discuss possible implications of these observations in the following sections.

A layered Earth model such as shown in Fig. 1 is an idealization. Deviations from a simplified layered model are sometimes important in the discussion of the Earth's structure and dynamics. First, significant lateral variations occur in both the crust and the mantle, reflecting the lateral variation of temperature and/or composition. Second, the structure of the Earth is sometimes anisotropic (anisotropy in the upper mantle is taken into account in a simplified way in the PREM). Studies of fine structure of the Earth (lateral heterogeneity and anisotropy) have made significant progress during the past few years as a result of the development of digital broad-band seismic networks and powerful computers. The results and their implications for the Earth's dynamics are discussed in Sec. 4.3.

**1.1.2 Solar Abundance and the Bulk Composition of Silicate Earth.** The Earth's internal constitution may also be studied by analysis of the chemical composition of rocks (geochemistry). Unfortunately, we only have access to rocks presently at the surface of the Earth. Rocks are there as a result of complicated processes of differentiation and tectonics and do not represent the average composition of the Earth. To get some insight into the composition of the deep interior of the Earth, we need some understanding of the source materials from which the Earth was formed and the differentiation processes that have occurred throughout its history.

The Earth was formed in the solar nebula at ~4.5 billion years ago. The Earth's present chemical structure is a result of differentiation processes that have occurred in the solar nebula and in the Earth's interior. Therefore, a starting point of understanding the chemical composition and the differentiation processes in the Earth (and in the solar nebula) is the chemical composition of the solar system ("solar abundance"). There are two ways of estimating solar abundance. The first way is through analysis of the chemistry of the outer layer of the sun where convection is vigorous and therefore the chemistry of the outer layer is believed to be representative of the average chemistry of the sun and of the solar system-

The second way is examination of the chemical composition of the "primitive" (meaning undifferentiated) meteorites such as (type I) carbonaceous chondrites. These two estimates agree well, except for some volatile elements which are depleted from chondrites. The average chemical composition of the non-volatile components of the solar system is given by the "solar abundance" in Fig. 3.

Basaltic magma is generated by partial melting of the upper mantle (see Secs. 1.2.1 and 3.2.1). Ringwood (1979) considered that upper mantle rocks or peridotites (composed mainly of olivine and pyroxenes) sampled as xenoliths by some volcanoes represent a residue of partial melting that generates basaltic magma. Therefore, the composition of the source material from which both basaltic magma and peridotite xenoliths are formed is considered to be some average of the two. This hypothetical source material is called "pyrolite" (see Fig. 3).

The chemical composition of upper-mantle rocks shows a large diversity due to variations in the degree of differentiation by partial melting. Rocks that show evidence of minimum differentiation may be representative of the primitive mantle. The composition of these primitive rocks is similar to that of pyrolite and has the following characteristics (Fig. 3):

1. Most of the refractory elements (except for elements with strong affinity to Fe, called siderophile elements) have abundances similar to the "solar abundance," although the Mg/Si ratio of the mantle (about 1.27 in atomic ratio) is slightly higher than that of the solar abundance (about 1.05);
2. Fe and siderophile elements are depleted; and
3. volatile elements are depleted.

Among the above compositional characteristics of the primitive upper mantle, 2 and 3 are readily explained by differentiation due to the formation of the Earth's core and by differentiation in the solar nebula, respectively. However, the origin of the high Mg/Si ratio [item (1)] has been a controversial matter. Three alternative explanations are possible:

1. The chemical composition of the Earth is different from the "solar abundance," possibly because of the differentiation processes in the solar nebula,

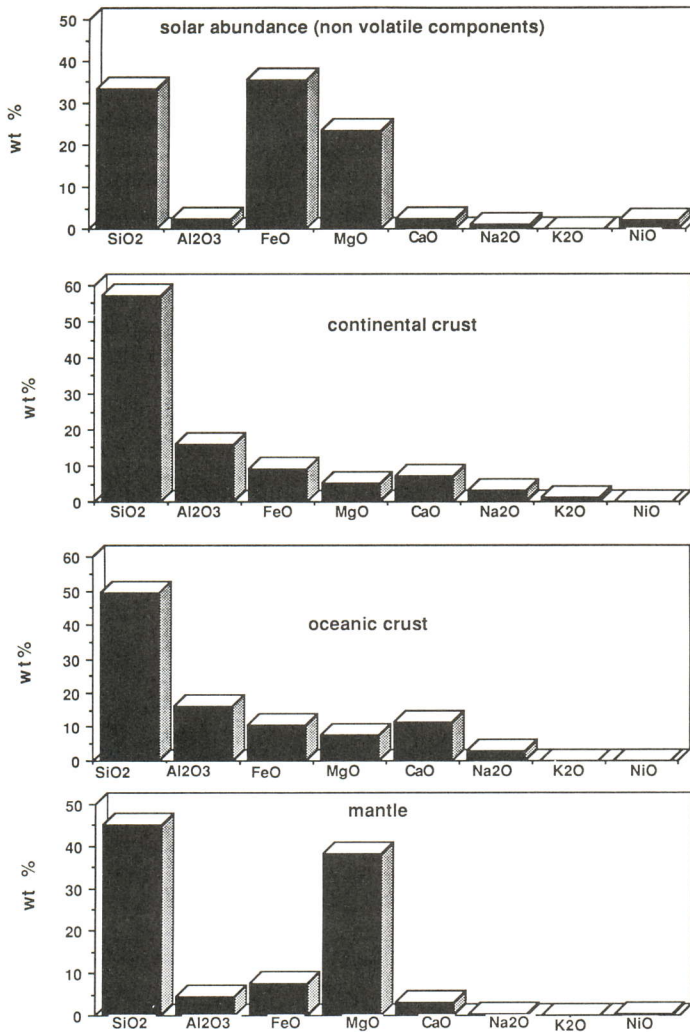


**FIG. 3.** The chemical composition of the solar system, the mantle (the pyro-lite model), and the oceanic and continental crust.

- the lower mantle (and/or the transition zone) is more enriched with Si than the upper mantle, and
- a significant amount of silicon is dissolved in the core.

## 1.2 The Composition of the Earth

(See also VOLCANICS; PLATE TECTONICS; GEOLOGY)

**1.2.1 The Crust.** The crust is the near-surface layer with variable thickness (~5–50 km). The crust in the oceanic region is considerably thinner than the crust in the continental region and is remarkably homogeneous with ~6-km thickness. In contrast, the thickness of continental crust is highly hetero-

ogeneous. It is 10–20 km in the Basin and Range province in the U.S.A., but it is ~50 km in Tibet.

The oceanic crust is made of sediments (major chemical composition being CaCO<sub>3</sub> and SiO<sub>2</sub>) and an underlying basaltic layer {basalt is a fine-grained rock composed mostly of calcium-rich feldspar (CaAl<sub>2</sub>Si<sub>2</sub>O<sub>8</sub>) and pyroxenes [(Mg,Fe,Ca)SiO<sub>3</sub>]}. The basaltic layer is created at mid-oceanic ridges by the partial melting of upper mantle rocks (see Sec. 3.2.1). The oceanic crust subducts together with the underlying uppermost mantle (together they constitute the oceanic lithosphere) into the deeper mantle at ocean trenches.

The continental crust is more heterogeneous than the oceanic crust, reflecting its

complicated history of metamorphism and deformation. A simplified model divides it into two layers: the upper and the lower continental crust. The upper continental crust is mainly composed of silica-rich rocks such as granitoids, the major constituent minerals being quartz ( $\text{SiO}_2$ ), potassium/sodium-rich feldspars  $[(\text{K},\text{Na})\text{AlSi}_3\text{O}_8]$ , biotite  $[\text{K}(\text{Mg},\text{Fe})_3(\text{AlSi}_3\text{O}_{10})(\text{OH})_2]$  and hornblende  $[\text{Ca}_2(\text{Mg},\text{Fe},\text{Al})_5(\text{Si},\text{Al})_8\text{O}_{22}(\text{OH})_2]$ . The lower crust is composed of more mafic (meaning MgO- and FeO-rich) rocks such as basalt, gabbro, or amphibolite, the major constituent minerals being calcium-rich feldspar, pyroxenes, hornblende, and amphibole  $[(\text{Mg},\text{Fe},\text{Ca},\text{Na})_{2,3}(\text{Mg},\text{Fe},\text{Al})_5(\text{Si},\text{Al})_8\text{O}_{22}(\text{OH})_2]$ .

**1.2.2 The Mantle.** The crust-mantle boundary is referred to as the Mohorovičić (or Moho) discontinuity. The velocity of compressional waves changes from 6–7 to 8 km/s at this discontinuity. The presence of clear reflection at this discontinuity indicates that this is a sharp boundary: The width must be significantly smaller than the wavelength of seismic waves ( $\sim 5$  km).

The mantle may be divided into three layers: the upper mantle ( $< 400$  km), the transition zone (400–670 km), and the lower mantle (670–2900 km).

**1.2.2.1 The Upper Mantle.** The layer below the Moho discontinuity down to  $\sim 400$  km is referred to as the upper mantle. The comparison of inferred velocities with laboratory measurements shows that the major constituent minerals are olivine, pyroxenes, and garnets  $[(\text{Mg},\text{Fe},\text{Ca})_3\text{Al}_2\text{Si}_3\text{O}_{12}]$ . Olivine is the most abundant mineral in the uppermost mantle. It has highly anisotropic elastic properties and the observed anisotropy of seismic waves in the upper mantle (see Sec. 4.3.2) can be explained by the anisotropic alignment of olivine. However, the relative amounts of these minerals may change with depth.

The inhomogeneity parameter defined by Eq. (8) has low values in the upper mantle, indicating that the temperature gradient is much higher than the adiabatic gradient. This is consistent with the temperature gradients estimated from other geophysical and petrological observations (see Sec. 2.1).

The high temperature gradient causes a mechanical stratification of the upper mantle (see also Sec. 4.2). The top cold part is the lithosphere which is characterized by high

velocity and low attenuation of seismic waves, low electrical conductivity, and high creep strength (viscosity). A layer beneath the lithosphere is characterized by relatively low velocity and high attenuation of seismic waves, high electric conductivity, and low creep strength, all of which are indicative of high temperatures (temperatures close to the melting temperature). This layer is called the asthenosphere. The lithosphere/asthenosphere boundary is well defined by a sharp change in physical properties, but the bottom of the asthenosphere is not well defined. The depth of the lithosphere/asthenosphere boundary varies from place to place. In the oceanic mantle, the lithosphere thickness increases with age: the lithosphere is very thin near the ocean ridges where new oceanic lithosphere is formed, but its thickness increases up to 50–100 km at the age of  $\sim 100$  million years.

An important issue about the asthenosphere is whether it represents a layer of partial melting or not. It was often postulated that the geophysical anomalies (low velocity and high attenuation of seismic waves, high electrical conductivity, low viscosity) in the asthenosphere are due mainly to the presence of a small amount of melt. But recent experimental studies on elasticity (and anelasticity), electrical conductivity, and rheology of upper-mantle rocks show that high temperature (and/or the presence of hydrogen) is sufficient to cause these anomalies. Partial melting may not be required throughout the asthenosphere but may be a localized phenomenon beneath volcanoes rather than a global phenomenon.

**1.2.2.2 The Transition Zone.** Laboratory studies under high pressures and temperatures show that silicate minerals undergo several series of phase transformations at the pressure and temperature conditions corresponding to those in the transition zone (400–670 km). Most of these phase transformations are of the first order and are associated with the increase in density and in seismic-wave velocities (see Table 2). The observed high gradients or discontinuities in density and in seismic-wave velocities (and the resultant high inhomogeneity parameter) in the transition zone is mostly attributed to these phase transformations.

Olivine  $[(\text{Mg},\text{Fe})_2\text{SiO}_4]$  with  $\text{Fe}/(\text{Fe} + \text{Mg}) \sim 0.1$  transforms to the modified spinel structure at  $\sim 400$  km and then to the spinel

structure at  $\sim 500$  km and finally to the perovskite  $[(\text{Mg,Fe})\text{SiO}_3] + \text{magnesiowüstite } [(\text{Mg,Fe})\text{O}]$  at  $\sim 670$  km (see Fig. 4). In these cases, the packing of atoms changes significantly in a narrow pressure (or depth) interval (see Fig. 4). The sharp increases in density and in seismic-wave velocities at  $\sim 400$  and  $\sim 670$  km are considered to be due mainly to the transitions from olivine to modified spinel and from spinel to perovskite + magnesiowüstite, respectively (the modified-spinel to spinel transformation does not change the density or velocity very much; see Table 2). In the case of the spinel to perovskite + magnesiowüstite transformation, the number of oxygen ions surrounding the silicon ions changes with the transformation: Silicon ions are surrounded by four oxygen ions in spinel, while they are surrounded by six oxygen ions in perovskite.

The other example is the transformation of pyroxene  $[(\text{Mg,Fe})\text{SiO}_3]$  into the garnet structure. In this case, the mutual solubility of pyroxenes and aluminosilicate garnet  $[(\text{Mg,Fe})_3\text{Al}_2\text{Si}_3\text{O}_{12}]$  increases with pressure. Thus the transformation is gradual and this phase transformation is considered to be responsible for the observed gradual increase in

density and velocities in the depth range of 400–670 km. In a silica-rich garnet, some lattice sites which are normally occupied with aluminum ions are occupied with silicon and magnesium ions, and therefore those silicon ions are surrounded by six oxygen ions. Garnets which have silicons surrounded by six oxygens are called majorite.

The transformation pressure  $P_{\text{tr}}$  varies with temperature through the Clausius–Clapeyron relation, viz;

$$\frac{dP_{\text{tr}}}{dT} = \frac{\Delta S}{\Delta V}, \quad (9)$$

where  $\Delta S = S_{\text{hpp}} - S_{\text{lpp}}$  ( $S_{\text{hpp}}$ , entropy of the high-pressure phase;  $S_{\text{lpp}}$ , entropy of the low-pressure phase) and  $\Delta V = V_{\text{hpp}} - V_{\text{lpp}}$  ( $V_{\text{hpp}}$ , volume of high-pressure phase;  $V_{\text{lpp}}$ , volume of low-pressure phase). In all cases,  $\Delta V$  is negative, but the sign of  $\Delta S$  depends on specific transformations. In the case of the olivine to modified spinel transformation,  $\Delta S$  is negative, that is, the modified spinel has smaller entropy than olivine, and hence  $dP_{\text{tr}}/dT$  is positive. In contrast, the phase transformation from spinel to perovskite + magnesiowüstite has negative  $dP_{\text{tr}}/dT$ , because the

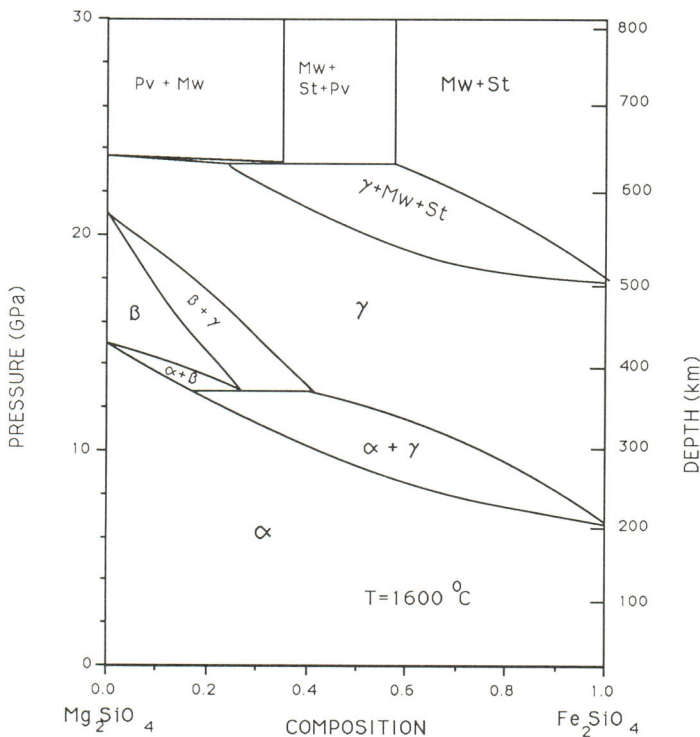


**FIG. 4.** The phase diagram of  $(\text{Mg,Fe})_2\text{SiO}_4$ .  $\alpha$ , olivine;  $\beta$ , modified spinel;  $\gamma$ , spinel; Pv, Perovskite; Mw, magnesiowüstite; St, stishovite. For a typical chemical composition appropriate to the Earth's interior [ $\text{Fe}/(\text{Mg} + \text{Fe}) \sim 0.1$ ],  $(\text{Mg,Fe})_2\text{SiO}_4$  transforms from olivine ( $\alpha$ ) to modified spinel ( $\beta$ ) at  $\sim 400$  km, to spinel ( $\gamma$ ) at  $\sim 500$  km, and finally to perovskite (Pv) + magnesiowüstite (Mw) at  $\sim 670$  km at  $T \sim 1600^\circ\text{C}$ .  $T \sim 1600^\circ\text{C}$  is the temperature estimated at 670 km on the basis of the comparison of the phase diagram with the seismological observations (see Sec. 2).



perovskite (+ magnesiowüstite) has higher entropy than spinel. Since the transformation pressure (depth) depends on temperature, by measuring the exact depth of phase transformations from seismological observations, one can estimate the temperature at these depths (see Sec. 2.3).

Although the major cause for high velocity gradients and velocity discontinuities in the transition zone is now known to be phase transformations in silicates, it is not well established whether the observed density and velocity changes in this region are solely due to phase transformations or partly due to some chemical stratifications as well. Seismological and petrological observations are also consistent with chemical stratification involving enrichments in pyroxenes and/or garnet in the transition zone.

Major seismic discontinuities in the mantle occur at  $\sim 400$  and  $670$  km on the global scale. However, these depths may vary laterally because of heterogeneity in temperature and/or chemistry (or mineralogy). In particular, large variation in these depths is expected in and around subducting slabs where a large lateral variation in temperature and/or chemistry (mineralogy) occurs. High-resolution seismological studies are under way to detect these fine details, which contain important information as to lateral variation in temperature and/or chemistry (or mineralogy) and hence have important clues as to the dynamics of the Earth's interior.

**1.2.2.3 The Lower Mantle.** The lower mantle is mostly composed of  $(\text{Mg,Fe})\text{SiO}_3$  perovskite and magnesiowüstite. The amount of magnesiowüstite is not well constrained and ranges from 0% to 20% depending on the models. Thus the  $(\text{Mg,Fe})\text{SiO}_3$  perovskite is the most abundant mineral in the Earth (it constitutes  $\sim 40\%$ – $50\%$  of the Earth). The velocity and density variations in the lower mantle are smooth, and are compatible with a homogeneous composition without major phase transformations except near the topmost lower mantle ( $\sim 670$ – $1000$  km) where relatively high gradients of these properties are observed. The phase transformation of majorite garnet into perovskite structure, or formation of some aluminous high-pressure minerals, may be responsible for the anomalous density and velocity gradient of the topmost part of the lower mantle.

**1.2.2.4 The  $D''$  Layer and the Core–Mantle Boundary.** The very bottom of the Earth's mantle ( $100$ – $200$  km thick), which is called the  $D''$  layer, has unusual physical properties: the velocity gradient is low and lateral variation is very large (Lay, 1989).

Two hypotheses have been proposed to explain this layer. One is that the  $D''$  layer corresponds to the bottom thermal boundary layer of a convecting mantle where the temperature gradient is high. The other alternative is that the  $D''$  layer is chemically different from the rest of the mantle. A high temperature gradient is also suggested by the comparison of estimated temperatures in the mantle with the melting temperatures of the core materials (see Secs. 2.3 and 3.3). Both high temperature gradient and large chemical heterogeneities may cause the unusual properties of the  $D''$  layer.

The core–mantle boundary is not smooth but has some topography with amplitude  $\sim 0.5$  to  $\sim 5$  km. Such topography may be a result of upwelling and downgoing convection current in the Earth's mantle and may also reflect the density variations due to chemical heterogeneities. The topography at the core–mantle boundary enhances the mechanical interaction of the core and mantle.

**1.2.3 The Core.** The core is divided into two parts: the outer core and the inner core. The densities of these two layers are much higher than those of silicates, and the major constituent of the Earth's core is believed to be metallic iron (Fig. 5). This conclusion is supported by the comparison of chemical compositions of the mantle (and the crust) with the solar abundance (Fig. 2). The inspection of Fig. 2 shows that the mantle (and the crust) is significantly depleted in iron compared to the solar abundance, suggesting an iron-rich layer in the deep portion of the Earth.

The absence of shear-wave propagation in the outer core indicates that it is largely in a molten state. This metallic liquid outer core may generate the geomagnetic field by convection. The observed density of the outer core indicates that the outer core is less dense than molten iron. Some light elements are needed to explain the observed density. Candidates include sulfur, oxygen, hydrogen, silicon, and carbon. High-pressure experiments show that all of these elements can be dissolved into iron at high pressures and high

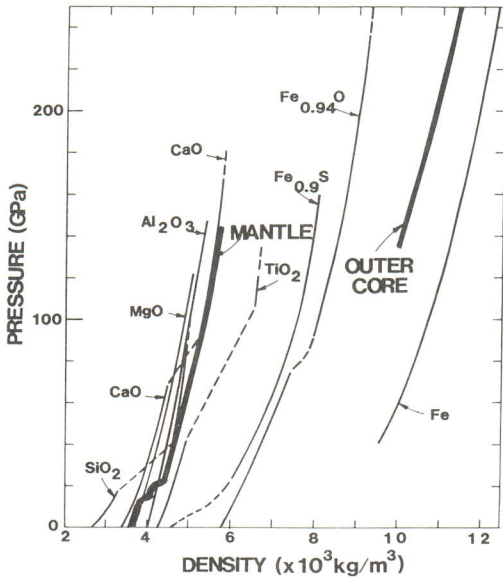


FIG. 5. Density–pressure relationships for various materials. Thin solid lines are those determined by laboratory experiments by shock waves. Thick solid lines are those inferred from seismological observations. The comparison shows that the mantle is composed of silicates or oxides but the core is composed mainly of iron.

temperatures. No consensus has been reached as to which of these elements are dominant. An important effect of light-element alloying is that it significantly reduces the melting temperature.

Shear waves pass through the inner core, and therefore it must be largely in a solid state. The density of the inner core is close to that of pure iron (+ nickel). Thus the Earth's core appears to be chemically layered: a relatively pure, solid inner core, and a liquid outer core containing a significant amount of light elements. An interesting hypothesis is that the inner core may have resulted from the solidification of the outer core as a result of secular cooling. On the basis of the seismologically determined density jump at the outer–inner core boundary and the assumption that the inner core has grown throughout the Earth's history, one can estimate the rate of energy release upon the solidification of the inner core. It is shown that the gravitational energy released by the growth of the inner core can provide sufficient energy to generate the geomagnetic field.

## 2. EARTH'S THERMAL REGIMES

### 2.1 Introduction

The temperature profile  $T(z)$  of the Earth's interior is determined by the heat generation and heat transfer processes through the energy conservation equation, viz;

$$\frac{\partial T}{\partial t} = \left( \frac{k}{\rho C_p} \right) \nabla^2 T + \frac{H}{\rho C_p} - \mathbf{v} \cdot \nabla T, \quad (10)$$

where  $k$  is thermal conductivity,  $C_p$  the specific heat,  $H$  the heat generation per unit volume, and  $\mathbf{v}$  the velocity. The first term in the rhs of Eq. (10) indicates the heat loss due to thermal conduction, the second term the heat generation, and the third term the energy transfer due to convection. The relative importance of each term depends on specific geological settings. For example, the heat production due to radioactive elements is important in the continental crust, but is less important in the oceanic crust and in the mantle. The relative importance of convective and conductive heat transfer depends on the rheology (viscosity) of Earth material (see Sec. 4). Convection becomes important when the Rayleigh number exceeds a critical value ( $\sim 10^3$ ). The Rayleigh number for a fluid layer heated from below is given by

$$Ra = \alpha \rho \Delta T g L^3 / \kappa \eta, \quad (11)$$

where  $\alpha$  is the thermal expansion,  $\Delta T$  the temperature difference between the top and bottom of the layer,  $L$  the thickness of the layer,  $\kappa$  the thermal diffusivity ( $\kappa = k / \rho C_p$ ), and  $\eta$  the viscosity. Among these parameters, the most critical is the viscosity, which changes significantly with temperature (and pressure) (see Sec. 4). The parameters in the equation are presented in Table 3 which shows that the Rayleigh number of the mantle (below the asthenosphere) is  $10^5$ – $10^7$  and therefore vigorous convection should occur in most of the mantle (and the core).

When convective heat transfer is not important, the temperature profile is determined by heat generation within a layer and by the boundary conditions [ $T$  and the heat flux  $J = k(dT/dz)$  at the boundary]. The amount of heat flux varies from place to place and ranges from  $(20 \text{ to } 300) \times 10^{-3} \text{ W m}^{-2}$ , and the total heat loss from the Earth is estimated to be  $\sim 4 \times 10^{13} \text{ W}$ . Since the thermal conductivities

**Table 3.** Physical constants and parameters relevant to mass and heat transfer in the Earth.

Thermal expansion $\alpha^a$	$3 \times 10^{-5}/\text{K}$
Acceleration of gravity $g^b$	$10 \text{ m}^2/\text{s}$
Density $\rho^c$	$(3-5) \times 10^3 \text{ kg}/\text{m}^3$
Thermal diffusivity $\kappa$	$10^{-6} \text{ m}^2/\text{s}$
Thickness of the layer $L^d$	400–2900 km
Viscosity $\eta^e$	
(asthenosphere and below)	$10^{20}\text{--}10^{22} \text{ Pa s}$
(lithosphere)	$10^{24} \text{ Pa s}$ or higher
Temperature difference $\Delta T^f$	1500–4000 K

<sup>a</sup> Thermal expansion in minerals depends on temperature and pressure. This value is for olivine at high  $T$  ( $T \sim 1000\text{--}1500 \text{ K}$ ) and at 0.1 MPa.

<sup>b</sup> The acceleration of gravity is nearly constant throughout the Earth's mantle.

<sup>c</sup> See the Earth model in Fig. 1.

<sup>d</sup> For the upper mantle,  $L = 400 \text{ km}$ ; for the whole mantle,  $L = 2900 \text{ km}$ .

<sup>e</sup> The viscosity of mantle materials is a strong function of temperature (and pressure) and varies significantly with depth (see Sec. 4; Fig. 9).

<sup>f</sup> See Sec. 2.

of rocks are generally small ( $0.1\text{--}0.5 \text{ W}/\text{m K}$ ), steep temperature gradients ( $10\text{--}500 \text{ K}/\text{km}$ ) will be formed in a layer where only conductive heat transfer occurs. In contrast, when convective heat transfer becomes important, the temperature profile within a convection cell becomes close to adiabatic ( $dT/dz = \alpha g T / C_p$ ), leading to a much smaller gradient ( $0.3\text{--}0.5 \text{ K}/\text{km}$  for the upper mantle). One expects therefore that the temperature gradient near the surface (i.e., the lithosphere) is much higher than in the deep mantle.

The temperature profile also varies laterally because the amount of convective heat transport and of heat generation varies from place to place. A large amount of heat is carried to the surface near ocean ridges by an upwelling convective current, but the downgoing current related to subducting slabs at ocean trenches will cool the mantle. The lateral variation in temperatures therefore reflects the convective pattern and provides useful constraints as to the dynamics of the deep interior of the Earth (see Sec. 4.3).

The Earth's temperature profile has also changed through geological time. Current understanding of temporal variation of the Earth's temperature is discussed in Sec. 2.4.

## 2.2 Heat Flow and Near-Surface Temperature Profile

The processes that determine the temperature profiles are quite different between the oceanic and the continental lithosphere. The oceanic lithosphere contains only a small amount of radiogenic elements and the temperature profiles are mainly determined by the heat flux carried by the underlying convective current. This heat flux is large near ocean ridges and decreases with the distance from ridges. Thus the temperature of the oceanic lithosphere decreases with the distance from ocean ridges. The temperatures near ocean ridges exceed the solidus of upper mantle rocks and partial melting occurs to create a basaltic layer.

In the continental lithosphere, the heat transported by the underlying convective current is relatively small [ $(30\text{--}50) \times 10^{-3} \text{ W m}^{-2}$ ] compared to the oceanic lithosphere. However, the contribution from radiogenic heat ( $H$ ) in the continental crust is significant and compensates the effects of relatively small heat flux. Thus the temperature profiles of the continental lithosphere are similar to those of old oceanic lithosphere, and the heat flux from the old oceanic lithosphere is similar to that from the continental lithosphere. In total, the heat flux from the Earth amounts to  $\sim 4 \times 10^{13} \text{ W}$ .

The temperature gradient measured in this way ranges from  $\sim 10 \text{ K}/\text{km}$  in the stable continent to more than  $500 \text{ K}/\text{km}$  near volcanic regions (such as ocean ridges). When extrapolated to deeper portions, temperatures would exceed the melting temperatures of most of rocks at the depth of  $100\text{--}200 \text{ km}$ . However, seismological observations indicate that most of the Earth's mantle is solid. The implication is that the temperature gradients at the deeper portions must be significantly smaller than the near-surface gradients.

## 2.3 Temperature Profiles of the Earth's Deep Interior

Melting temperatures of Earth materials (see Sec. 3) provide important constraints on the temperature profiles. First, the temperatures in the inner core and the mantle must be lower than the melting temperatures of the relevant materials. Second, the temperatures

in the outer core must be higher than the melting temperature of iron (plus some light elements).

Melting temperatures of iron (and its alloys) have been determined up to pressures corresponding to the core pressures, using shock waves as well as static compression experiments. The melting temperature of iron increases with pressure and reaches  $\sim 7000$  K at the pressure of the outer-inner core boundary. If the core were made of pure iron, this temperature would be the temperature at the outer-inner core boundary. However, the outer core contains a significant amount of secondary components such as sulfur, oxygen, and hydrogen (see Sec. 1.2.3) which, in most cases, reduce the melting temperature. For example, if the light element is sulfur, the melting temperature for the eutectic composition will be  $\sim 4500$  K at the outer-inner core boundary and  $\sim 3500$  K at the core-mantle boundary (Jeanloz, 1990).

In addition to these broad constraints, more detailed estimates of temperature profiles can be made using petrological studies of mantle xenoliths (fragments of rocks carried up by volcanoes) and from the phase diagrams determined by high-pressure experiments (see Sec. 1.2.2.2). Also, some physical properties such as electrical conductivity or seismic-wave velocities (see Sec. 1.1.1, Fig. 2) can be used to estimate the temperature profiles in the deep interior of the Earth. The temperatures in the upper mantle and the transition zone have been estimated using these techniques (Fig. 6) (Jeanloz and Morris, 1986). The following points can be noted.

1. The temperature gradient changes from steep in the upper portion of the mantle to gradual in the deeper portion. The temperature gradient in the deeper mantle (400–670 km and below) thus estimated is close to the adiabatic gradient (0.3–0.5 K/km).
2. The temperature in the upper mantle be-

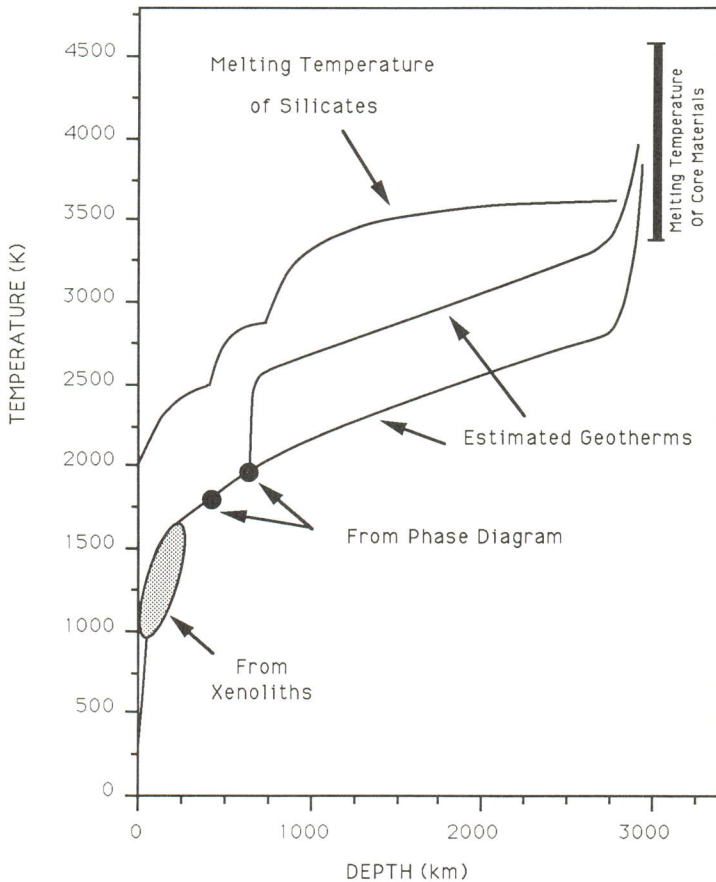


**FIG. 6.** Average temperature profiles for the Earth's interior. Shown together are the depth variation of melting temperatures of silicates and the melting temperature of iron at the core-mantle boundary determined by laboratory experiments. The two curves in the lower mantle show two possible temperature profiles, one (colder one) corresponding to whole-mantle convection, the other (hotter one) corresponding to layered convection with a thermal boundary layer at  $\sim 670$  km.

low young ocean is higher than the temperature in a stable continent, but they are indistinguishable when the age of the ocean exceeds  $\sim 100$  millions years.

When the temperature at  $\sim 670$  km ( $\sim 2000$  K) is extrapolated to the core–mantle boundary assuming an adiabatic gradient (as suggested by the seismic-wave velocities in the greatest part of the lower mantle), one gets the temperature of  $\sim 2500$ – $3000$  K, which is lower than the melting temperature of the core materials ( $4000 \pm 500$  K). The implication is that there must be some layers in the Earth below 670 km where the temperature gradient is significantly higher than the adiabatic gradient. Possibilities include thermal boundary layers near 670 km and/or at the bottom of the mantle ( $D''$  layer).

The uncertainties in estimated temperatures become larger as we go deeper in the Earth. The uncertainties in the estimated temperatures in the upper mantle and transition zone are  $\sim \pm 100$  K. The major uncertainty in the temperatures in the lower mantle concerns the presence or absence of thermal boundary layers in the transition zone and this yields  $\sim \pm 500$ -K uncertainties in the estimated temperatures. The uncertainties in the temperatures in the core come from the uncertainties in the melting temperature of core materials and are more than  $\pm 1000$  K.

## 2.4 Thermal History

The previous discussions are concerned mainly with the Earth's present temperature profiles. The Earth's temperatures, however, have changed with time since the rates both of heat generation and of heat loss change with time. The major energy sources for the Earth's dynamics are gravitational energy and the heat produced by radiogenic elements. A significant amount of gravitational energy was released during the early stage of evolution of the Earth (during accretion and core formation) and probably throughout geological history as a result of growth of the inner core. The amount of gravitational energy released during accretion is proportional to  $R^5$  ( $R$  is the radius of the planet), and therefore the bigger the planet, the larger this effect. The net temperature increase due to gravitational energy depends also on the rate of energy release and the efficiency of heat loss. When a

planet is formed quickly, the heat is largely retained in the planet and a significant temperature increase will occur. Also, when a planet has a thick atmosphere, it will reduce the efficiency of energy loss and increase the temperature. Current theoretical studies on the formation processes of Earth suggest that a significant melting leading to the formation of a magma ocean may have occurred during the accretion and the core-formation processes.

The heat production due to radiogenic elements is determined by their concentration and the half-life times. Important radiogenic elements include  $^{235}\text{U}$ ,  $^{238}\text{U}$ ,  $^{232}\text{Th}$ ,  $^{40}\text{K}$  and possibly  $^{26}\text{Al}$ .  $^{26}\text{Al}$  has a short half-life (0.74 million years) and it may have been important in the early stage of the solar nebula. All of other elements have half-lives on the order of a billion years and their activity has been decaying slowly.

The time variation of the Earth's average temperature  $T$  is determined by the balance of heat generation and heat loss as

$$\rho C_p V \frac{dT}{dt} = H^+(t) - H^-(t), \quad (12)$$

where  $\rho$  is the density,  $C_p$  the specific heat,  $V$  the volume of the Earth, and  $H^+$  and  $H^-$  the rates of heat generation and heat loss, respectively. The present-day energy loss rate can be estimated from the heat-flow measurements (see Sec. 2.2) to be  $\sim 4 \times 10^{13}$  W. The heat generation due to radioactivity at present can be estimated if the bulk composition of the Earth is assumed to be the same as a primitive chondrite (see Sec. 1.1.2), which yields  $\sim 2 \times 10^{13}$  W. The imbalance between the two indicates that the Earth has been cooling through time. Both the release of gravitational energy and the heat production due to radiogenic elements were more significant in the early stage than they are today. Thus the temperature in the past should have been higher than it is now. However, the rate of temperature change is also controlled by the energy loss mechanisms. The most important energy loss mechanism is the convective heat transfer through the mantle (see Sec. 4). The efficiency of heat loss due to this mechanism depends on temperature because the viscosity of rocks depends strongly on temperature (see Sec. 4.2): the higher (lower) the temperature, the higher (lower) the rate of cooling.

In this way, the temperature-dependent viscosity of rocks tends to stabilize the temperatures in the Earth. Thus a rather moderate temperature drop of  $\sim 100\text{--}300\text{ K}$  is estimated from the Archean ( $< 2.5$  billion years) to the present.

### 3. MELTING OF SILICATES AND MAGMATISM

(See also VOLCANICS)

#### 3.1 Melting and Chemical Stratification

Melting is a very efficient way to create chemical stratification of the Earth. The major chemical boundaries of the Earth, namely the crust–mantle boundary, the mantle–core boundary, and the outer–inner core boundary, are considered to have been formed through some processes involving melting. Melting can create chemical stratification in two different ways. First, when partial melting occurs, melt may migrate up or down depending on its density relative to the host solid rock. Second, when total melting occurs, fractional crystallization in a melt will create a chemical stratification. The former process is believed to be responsible for the major volcanic activity near the surface, including that at mid-ocean ridges. The latter is believed to occur at the inner and outer core boundary and in magma chambers (or the hypothetical magma ocean).

When partial melting (or fractional crystallization from melt) occurs, selective enrichment or depletion of some elements occurs in the melt (or the solid phases). The nature of element partitioning between melt and solid phases depends strongly on the crystal structure of the solid phases and the degree of partial melting (or crystallization). Thus the measurements of abundance patterns of various elements in rocks provides important information as to the degree of melting (or crystallization) and the crystal structure of solid phases involved (and hence the depth of melting).

The melting temperatures of most Earth materials increase with pressure (Fig. 6). However, the rate of increase in melting temperature within the stability field of a given phase becomes small at high pressures because of the large increase in density of melt relative to solid (melts are more compressible

than solids). Secondary components sometimes have important effects on melting. An example is the effect of water on the melting of silicates: Water dramatically reduces the melting temperature and changes the chemical composition of the melt.

#### 3.2 Magmatism and Melting of the Earth's Interior

**3.2.1 Mafic Magmas.** Magmas enriched in  $(\text{Mg,Fe})\text{O}$  are called mafic magmas, and the typical one is basaltic magma. The most important igneous rock formed by the solidification of this type of magma is mid-ocean ridge basalt (MORB), and its production rate is approximately  $\sim 4.5\text{ km}^3/\text{year}$ . MORB comprises a major part of the oceanic crust that descends into the deep interior of the Earth at a subduction zone.

Some ocean islands such as Hawaii are composed of a somewhat different igneous rock called ocean island basalt (OIB), which shows enrichment in incompatible elements (elements that are selectively concentrated into the liquid phase upon partial melting). These rocks are thought to have originated in relatively undepleted regions (or mantle enriched in incompatible elements). In most cases, the volcanoes which supply these basalts remain at the same position for a geologically long period of time, while the surface plates move a significant distance. Thus these volcanoes are often referred to as "hot spots." The production rate of this type of magma is  $\sim 0.1\text{ km}^3/\text{year}$ .

**3.2.2 Silicic and Intermediate Magmas.** Magmas enriched with silica (e.g., granite) are called silicic, and magmas with a composition between silicic and mafic are called intermediate. Andesite is a typical igneous rock formed by an intermediate magma. These magmas are formed in the island arcs or the active continental margins, and they are generated by partial melting of the crust or the mantle in the presence of water. Silicic and intermediate magmatism is responsible for the growth of continents and island arcs. The production rate is  $\sim 1\text{ km}^3/\text{year}$ .

**3.2.3 Ultramafic Magmas and Melting in the Deep Mantle.** Komatiite is a unique igneous rock formed by the solidification of magmas which are extremely enriched in

(Mg,Fe)O (ultramafic magma). They occur mainly in the Archean period (more than ~2.5 billion years ago). Magmas with this composition indicate a high degree of partial melting and therefore high temperatures in the Archean period.

Theoretical studies of thermal history (see Sec. 2.4) strongly suggest extensive melting in the early stage of the Earth. Large-scale melting in the early stage of Earth's history could have generated a thick layer of ultramafic magmas (magma ocean). The consequences of such extensive melting can be inferred from experimental studies on melting at high pressures, and the results can be compared with geochemical and geophysical observations to shed some light on the degree of chemical differentiation in the Earth.

Melting experiments under ultrahigh pressure indicate that the chemical composition of the upper mantle is similar to the composition of partial melt that is formed at high pressures (13–15 GPa) and that the solidus phase (a solid phase that crystallizes first from the melt upon cooling) changes from olivine at low pressure to majorite at ~15 GPa, and finally to perovskite at ~25 GPa. Partial melting or crystallization involving majorite or perovskite results in quite different (trace) element partitioning than those involving upper mantle minerals (such as olivine or pyroxenes). Therefore some stratification, in both trace- and major-element chemistry, might have been formed in the mantle if large-scale melting had occurred in the early stage of Earth's history.

Another important observation in ultrahigh-pressure melting is that the density differences between melt and solid become smaller at high pressures. This eventually leads to density crossover: Melts will become denser than solids. If this density crossover occurs in the Earth, the transport of magmas from deep interior of the Earth would become difficult.

The consequences of large-scale melting (such as magma ocean) for chemical stratification depend on the processes of melt crystal separation as well as on the density contrasts and the partitioning of elements between melts and crystals. It has often been assumed that large-scale melting inevitably results in chemical stratification, but recent theoretical studies suggest that very limited chemical stratification might result because of a stirring effect of vigorous convection in the magma ocean.

## 4. EARTH'S RHEOLOGICAL STRUCTURE AND DYNAMICS OF THE EARTH'S INTERIOR

(See also PLATE TECTONICS)

### 4.1 Time-Dependent Deformation of the Earth

The Earth's dynamics is governed by the balance of the driving force determined by the density heterogeneity and the resistance force determined by rock rheology. The Earth's rheological properties depend on time scales and on the stress magnitude. At short time scales and for small deviatoric stresses, Earth materials behave like an elastic solid (with minor energy dissipation). When the time scale and/or the stress magnitude are large, nonelastic deformation will result, leading to permanent deformation that causes tectonic activities such as mountain building and earthquakes. The transition conditions from elastic to nonelastic therefore involve two criteria, the time-scale criterion and the stress criterion (Fig. 7).

To understand this, we must first understand the two contrasting mechanisms of nonelastic deformation. The first one is brittle deformation, that is, fracture. Fracture occurs mostly along a fault, and therefore the fracture strength of rocks is determined by the resistance for sliding along a fault. The strength  $\sigma$  of a rock in the brittle regime is given by

$$\sigma = \sigma_0 + \mu_f \sigma_n \quad (13)$$

where  $\sigma_0$  is the cohesive strength,  $\mu_f$  the friction coefficient, and  $\sigma_n$  the normal stress on the fault. Laboratory studies show that both  $\sigma_0$  and  $\mu_f$  are relatively independent of rock type, temperature, pressure, and strain rate. However, the strength in a brittle regime increases with pressure, since  $\sigma_n$  is proportional to pressure.

The second mechanism is ductile deformation. Ductile deformation occurs, in most cases, through the motion of crystalline defects in minerals. The motion of these defects is thermally activated, and therefore ductile deformation is important only at high temperatures. The easiness of the motion of defects depends on the strength of chemical bonds and crystal structure, and therefore the ductile strength depends on the rock type. To a first approximation, the dependence on rock

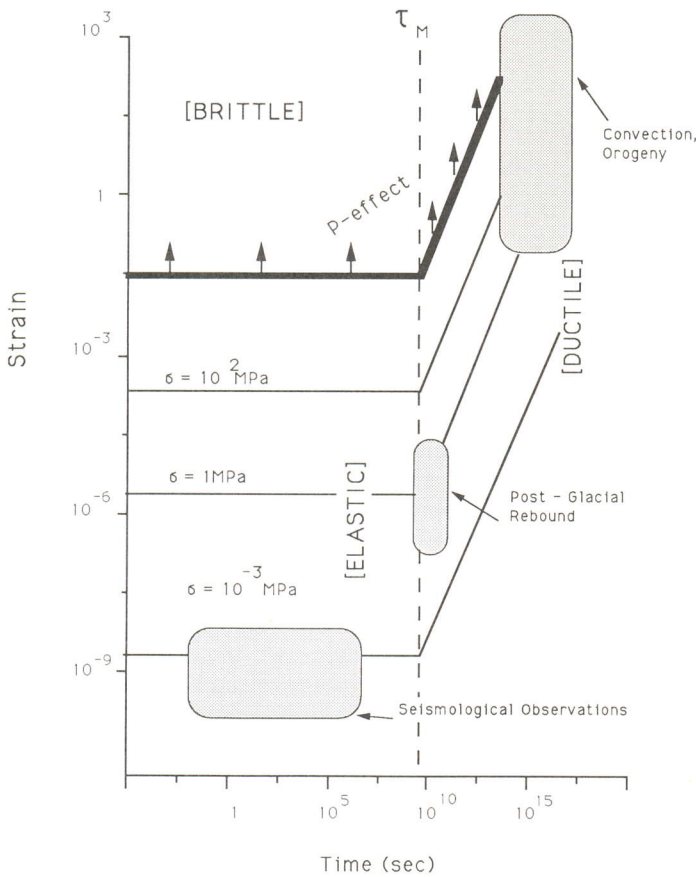


**FIG. 7.** Mechanical behavior of rocks as a function of time scales and strain (stress) magnitude. Constant stress contours are also shown for both elastic and ductile regimes. When the stress magnitude exceeds a critical value, a material will deform in the brittle manner (fracture), and this critical stress increases with pressure ("P-effect"); the critical stress shown in this figure corresponds to the stress in the continental lower crust and the uppermost mantle. Ductile deformation is important compared to elastic deformation when the Maxwell time  $\tau_M = \eta/\mu$  ( $\eta$ , viscosity;  $\mu$ , rigidity) is smaller than the time scale of the relevant process. The Maxwell time depends on temperature and pressure and the value shown in this figure is for the typical asthenosphere. Shown together are the strain magnitudes and time scales of typical deformation processes in the Earth.

type is through the melting temperature, and the flow law is given by

$$\dot{\epsilon} = A\sigma^n \exp[-\beta T_m(P)/RT], \quad (14)$$

where  $\dot{\epsilon}$  is the strain rate,  $\sigma$  the differential stress,  $A$  a constant preexponential factor,  $n$  the stress exponent ( $n=1-5$ ),  $T_m(P)$  the melting temperature which depends on pressure, and  $\beta$  a nondimensional constant. The effective viscosity  $\eta$  is defined by

$$\eta = \sigma/\dot{\epsilon}. \quad (15)$$

For Newtonian rheology (i.e.,  $n=1$ ), the effective viscosity is independent of stress, whereas for non-Newtonian rheology ( $n > 1$ ), the effective viscosity decreases with the stress magnitude. Ductile deformation is important compared to elastic deformation when the Maxwell time

$$\tau_M = \eta/\mu \quad (16)$$

is smaller than the time scale of deformation, where  $\mu$  is the rigidity. Thus ductile deforma-

tion is important in slow processes and/or at high temperatures (see Fig. 7).

Ductile deformation results in changes in rocks' microstructures reflecting deformation conditions. They include the formation of preferential alignment (preferred orientation) of minerals and the creation of crystal dislocations. The preferential alignment of minerals can be observed as an anisotropy in seismic-wave velocities as well as in thin sections of rocks under a microscope. The density of crystal dislocations and some other microstructures can be observed by the analysis of rock specimens and provide an estimate for the magnitude of differential stress in the Earth.

Brittle and ductile deformation are largely independent, and the lower of the strengths associated with these processes will determine the real strength. Thus the mechanical properties of rocks can be summarized as in Fig. 7. At low stresses and short time scale (or low temperatures), rock behaves as an elastic



solid. At high stress and short time scales (or low temperatures), rocks deform in a brittle manner. Finally, at long time scales (or high temperatures), rocks deform in a ductile fashion.

#### 4.2 Earth's Rheological Stratification

The Earth's rheological stratification can be predicted on the basis of temperature profiles (Fig. 6) and the constitution and the mechanical properties of rocks [Eq. (14)]. The temperature is low in the near-surface regions of the Earth, and therefore rocks are elastic or brittle depending on the stress levels. The strength of rocks in the near-surface layer increases with depth as a result of increases in pressure. As one goes to deeper portions, temperatures will increase, and this enhances ductile deformation. The depth of onset of ductile deformation depends on the rock type and the temperature profile. In the continental lithosphere, the lower crust will be a ductile layer with strength significantly smaller than that of the upper crust and the uppermost mantle. In the oceanic region, the crust is mostly a brittle layer and ductile deformation occurs only in the upper mantle. The ductile strength of the upper mantle first decreases with depth because of the rapid increase in temperature in near surface regions (Fig. 6). However, the temperature gradient becomes small at the deeper portions, and then the pressure effect (through the pressure dependence of melting temperature) becomes more important, which increases the ductile strength with depth. Thus one expects a strength minimum at depths where the

temperature gradient changes from a near-surface high gradient to a low gradient at the deeper portions (this depth depends on the temperature profile and is  $\sim 50$ – $200$  km in the oceanic mantle; see Fig. 6). At even deeper portions where a series of phase transformations occur in major constituent minerals, rheological properties will also change. Recent laboratory studies suggest that the garnet and spinel-rich transition zone (400–670 km) presumably has a larger viscosity than the olivine-rich upper mantle or the perovskite-rich lower mantle. Thus a rheological stratification of the Earth is a natural consequence of temperature and pressure distribution and of the phase transformations in the Earth.

The Earth's rheological properties can be inferred from some geological and geophysical observations. Attenuation of seismic waves provides information as to the Earth's non-elastic properties at relatively short time scales ( $1$ – $10^3$  s). The attenuation of seismic energy is measured by a quality factor  $Q$  defined as

$$Q^{-1} = \Delta E / 2\pi E, \quad (17)$$

where  $\Delta E$  is the energy dissipated per unit cycle, and  $E$  is the energy stored per unit cycle. Figure 8 shows the depth variation of  $Q$  in the mantle which is characterized by a high- $Q$  (low-loss) lithosphere (0–100 km), low- $Q$  (high-loss) asthenosphere (100–200 km), and a moderate- $Q$  lower mantle.

Time-dependent deformation after the last deglaciation provides the most detailed information as to Earth's rheological stratification. The melting of polar ice sheets  $\sim 10$  000 years ago changed the distribution of surface load,

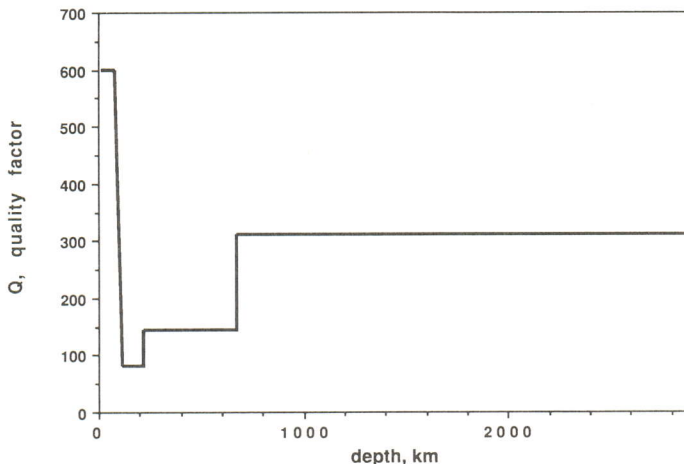
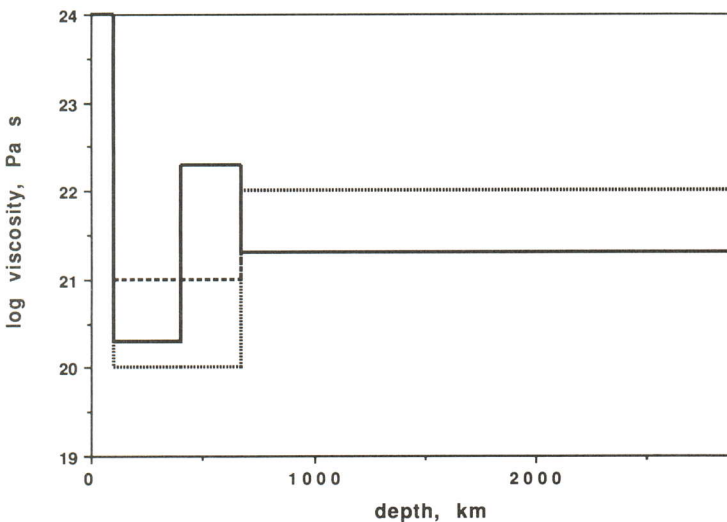


FIG. 8. Depth variation of seismic wave attenuation ( $Q$ , quality factor).

which induced plastic flow in the Earth. The resultant deformation is still going on today as observed by the change in sea levels at the coast or by the change in the spin rate of the Earth (as a result of change in the moment of inertia due to internal mass redistribution). Theoretical analyses of such deformation show that the near-surface layer of the Earth behaves like a thin elastic shell (the lithosphere), whereas the deeper portions behave like a viscous fluid.

Another observation related to mantle rheology is the geoid anomalies (anomalies of the height of equipotential surface of the Earth's gravity field). Such anomalies reflect the anomalies of mass distribution in the Earth. Mass anomalies with a long wavelength are supported by viscous flow and therefore provide a clue as to the rheological properties of the Earth's interior. Theoretical analysis of the geoid anomalies associated with subduction of the oceanic lithosphere suggests a significant increase in viscosity in the deep part of the mantle.

Most of these studies assume Newtonian rheology [linear relationship between strain rate and stress, i.e.,  $n=1$  in Eq. (14)]. The viscosity of the mantle thus inferred is shown in Fig. 9. The average viscosity of the Earth's mantle is well constrained from these studies ( $\sim 10^{21}$  Pa s), but the depth variation is poorly resolved. There are some indications that the asthenosphere has lower viscosity and the transition zone and the lower mantle have higher viscosity than the average.



**FIG. 9.** Depth variation of viscosity of the mantle. The three curves are the viscosity-depth profiles consistent with various time-dependent deformation (such as post-glacial rebound and geoid anomalies), and show the range of uncertainties involved in these studies. Average viscosity of the mantle is determined to be  $\sim 10^{21}$  Pa s by the analysis of the post-glacial rebound. The existence of a low-viscosity layer at  $\sim 100$ – $200$  km and of relatively high-viscosity layer(s) in the deep mantle are suggested by laboratory studies and from the analysis of geoid anomalies. However, the viscosities in the deep mantle (below 400 km) are poorly constrained.

### 4.3 Dynamics of the Earth's Interior

**4.3.1 Plate Tectonics (see also PLATE TECTONICS).** The estimation of the Rayleigh number defined by Eq. (11) for the Earth's mantle shows that it significantly exceeds the critical number ( $\sim 10^3$ ), for both the upper (or the lower) and the whole mantle (see Sec. 2.1). Thus the Earth's mantle must convect vigorously. The relative motion of the near-surface layer (lithospheric plates) is the manifestation of mantle convection. Several geophysical or geological observations indicate that Earth's surface is divided into several plates which move relative to each other with the speed of 1–10 cm/year. A lithospheric plate has a large creep strength at the Earth's surface, and deformation within a plate is minor except for continental collision zones such as Tibet. Most of the geological or geophysical processes such as earthquakes, volcanism, and mountain building occur at the boundaries of plates.

Plates that carry mostly oceans (such as the Pacific plate) are created at ocean ridges and subduct into the Earth's deep interior at ocean trenches. Subducting plates are marked by the planar zone of high seismic activity called the Wadati-Benioff zone which extends to  $\sim 700$  km in some areas (e.g., beneath the Japan, Tonga, and Kermadec trenches).

**4.3.2 Seismic Tomography and Deep-Mantle Dynamics.** Although the surface motion of plates is well established, the relation between plate motion and mantle convection is

not well known. One of the major issues is the depth extent of subduction and the style of mantle convection. One hypothesis is that the subducting slabs penetrate into the lower mantle and the convection occurs in a single cell as a whole mantle. The other alternative is that the subducting slabs do not penetrate deeper than  $\sim 700$  km, implying that the upper mantle (including the transition zone) and the lower mantle convect separately.

One of the powerful ways to distinguish these hypotheses is to study the fine structure of the mantle using seismological techniques. This is called seismic tomography, in which fine details of three-dimensional structures of the Earth can be revealed. In seismic tomography, deviation from a simplified layered Earth model such as PREM is mapped. There are two different types of deviations: lateral heterogeneity and anisotropy.

The lateral variations of temperature and chemistry are the most likely causes of lateral heterogeneities. When the major source of lateral heterogeneity is the heterogeneity in temperature, low velocity reflects high temperature and high velocity reflects low temperature.

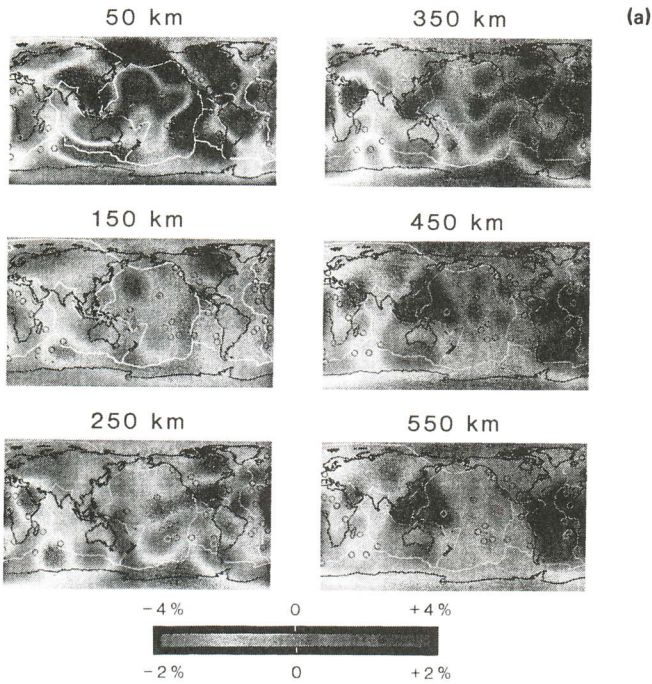
The correlation of lateral heterogeneity with tectonic setting is clear in the shallow portions [Plate I(a)]. Ocean ridges and young oceanic lithosphere show up as low-velocity anomalies, and old continents such as North America and Africa show up as high-velocity anomalies. The origin of velocity anomalies in the deep portions is not clear, but an important example is the depth extent of subducting slabs [Plate I(b)]. A cold slab is expected to show up as a high-velocity anomaly. The recent studies on slab penetration suggest that slabs do penetrate deep into the lower mantle in some areas (e.g., Kamchatka-Kuril) but they are deflected at the  $\sim 670$ -km boundary and do not penetrate into the lower mantle in other areas (e.g., under the Izu Bonin island arc in western Pacific).

Another fine structure that is related to Earth's dynamics is anisotropy. Most minerals have anisotropic elastic properties, and therefore if they are aligned nonrandomly in a rock, the rock will show anisotropy. Such anisotropy was first observed in the oceanic upper mantle in 1960s and was interpreted in terms of the preferential alignment of olivine as a result of mantle flow related to plate tectonics. Such studies have been extended

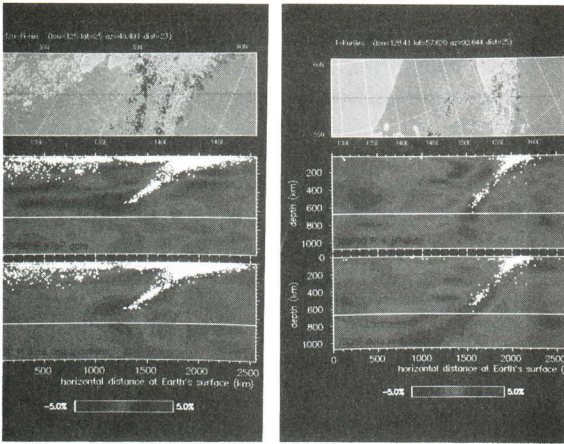
during the past few years to probe the anisotropy in the deeper portions of the Earth and on a global scale. In most cases, the direction of the fast seismic-wave velocity in the upper mantle is parallel to the flow direction. Therefore an anisotropy map such as Plate I(c) is considered to show the pattern of mantle convection.

Computer modeling of mantle convection plays an important role in the study of mantle dynamics. The equation of motion of a viscous fluid (Navier-Stokes equation) for a given set of material parameters (such as viscosity, density, and thermal expansion) may be solved with appropriate boundary conditions. The results of such studies can be used to predict possible convection patterns for a given set of material parameters and boundary conditions. Alternatively, such calculations may be used to put constraints on some material parameters such as depth variation of viscosities, by comparing the predicted results for various parameter sets with geophysical observations. These studies indicate that the material properties such as viscosity vary significantly with depth and that these variations in physical properties with depth have critical effects on the convection pattern.

**4.3.3 Geochemical Observations on Mantle Heterogeneities.** The best documented large-scale chemical heterogeneity of the Earth's mantle is the differences in trace-element abundance pattern between the source of the mid-ocean ridge basalt (MORB) and ocean island basalt (OIB). MORBs' trace-element abundance pattern shows that they originate in a region where incompatible elements are depleted. This indicates that MORBs are formed by the partial melting of rocks that have already undergone significant differentiation. In contrast, OIBs originate from a region which is enriched (or undepleted) in incompatible elements. Geochemical observations also indicate that these two regions have been separate for the time scale of a billion years. However, geochemical observations do not tell where these source regions are located. One possibility is that the depleted region corresponds to the upper mantle, and the undepleted region to the lower mantle. An alternative hypothesis is that these two regions are mixed like raisin bread, and that the mantle is homogeneous on the large scale.

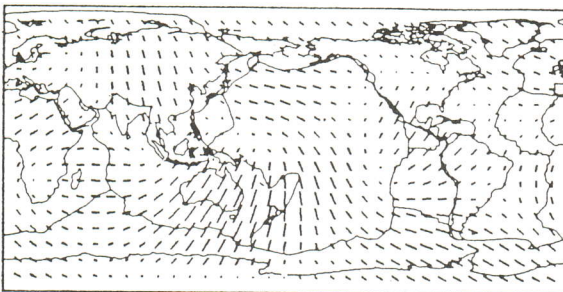


(a)



(b)

**PLATE 1.** Some results of seismic tomography. (a) Global maps of lateral heterogeneity of seismic wave velocities (distribution of anomalies in shear wave velocities at various depths in the upper mantle and transition zone; from Dziewonski and Woodward, 1991). Note that the scale for the velocity anomalies varies with depth. (b) Anomalies of compressional wave velocities in the vicinities of subduction zones (Izu-Bonin and Kurile). Top, locations of earthquakes; middle and bottom, velocity anomalies based on two different standard models together with the foci of earthquakes (shown by white dots) (van der Hilst *et al.*, 1991). High velocity anomalies (i.e., a subducting slab) appear to be deflected horizontally at ~670 km in the Izu-Bonin arc but they seem to be continuous down to ~1000 km in the Kurile arc. (c) Anisotropy of Rayleigh-wave (with period 167 sec) velocities in the asthenosphere. The directions of the bars indicate the directions of the fast Rayleigh waves, which is parallel to the orientation of convective motion (Montagner and Tanimoto, 1990).



(c)

— 2 percent

The whole-mantle convection is consistent with the latter idea, whereas the layered-mantle convection is consistent with the former idea.

While the chemical heterogeneity is evident in incompatible elements, the abundance pattern of compatible elements (Mg, Si, Ca, Al, Ti, and heavy rare-earth elements) of mantle xenoliths, sources of MORBs and OIBs, show little heterogeneity. This indicates that major fractionation involving melting in the transition zone or in the lower mantle did not occur, or else vigorous convective mixing occurred after or during the differentiation.

## 5. SUMMARY

The Earth is a chemically differentiated and dynamically evolving planet. The most significant differentiation processes are the formation of the crust and the core. The crust is composed of silica-rich rocks, the core is composed mainly of iron-rich alloys, and the mantle is composed of (Mg,Fe)O–SiO<sub>2</sub> rich rocks. There are some fine details in the structure of each layer, an important example of which is the discontinuities in the mantle at 400- to 670-km depth range. High-pressure experiments show that most silicate minerals undergo a series of phase transformations at this depth range. Thus a significant part of these discontinuities is due to phase transformations. A remaining question is whether all of these discontinuities are attributed to the phase transformations or some of them are due to changes in chemical composition. Geophysical and geochemical studies are under way to solve this problem.

The Earth is stratified also in terms of rheological properties: strong near-surface layer (lithosphere), solid but relatively weak underlying mantle, liquid outer core, and solid inner core. Convection occurs both in the mantle and in the outer core (and presumably in the inner core). Convection in the mantle is responsible for plate tectonics, and convection in the outer core is responsible for the generation of the geomagnetic field. The nature of convection in the mantle is determined by the balance of the driving force and the resistance force for convection, both of which are determined by the physical properties of rocks such as density and rheological

properties. These physical properties change significantly with depth as a result of phase transformations and the increase in pressure and temperature, leading to complicated convective motion in the Earth. A realistic picture of convective motion in the mantle is beginning to be inferred through the development of geophysical (seismic tomography) and geochemical observations combined with materials science studies of the properties of minerals under high pressures and temperatures.

## GLOSSARY

**Adams-Williamson Equation:** The equation that describes the compression of a homogeneous body in a gravity field.

**Archean:** The period earlier than 2.5 billion years in the Earth's history. The earliest period from 4.6 to 4.0 billion years ago is sometimes called Hadean. If we adopt this classification, the Archean is defined as the period from 4.0 to 2.5 billion years.

**Asthenosphere:** A soft layer below the lithosphere (50- to 200-km depth).

**Basalt:** A fine-grained, mafic igneous rock composed largely of plagioclase feldspar and pyroxenes.

**Brittle Deformation:** Deformation due to fracture. Brittle deformation occurs at low temperatures and/or low pressures.

**Carbonaceous Chondrite:** One type of meteorite, which is mainly composed of silicates. It contains various minerals that are chemically in disequilibrium. This type of meteorite is believed to be the most primitive material in the solar system.

**Ductile Deformation:** Deformation due to plastic flow. Ductile deformation of rocks occurs mostly at high temperatures (and high pressures).

**Geoid:** The equipotential surface of the Earth's gravity field.

**Incompatible Elements:** The elements which tend to be partitioned into magmas relative to coexisting minerals upon partial melting. These elements are not accommodated in lattice sites of the minerals because of mismatching of the ionic radii with the lattice site.

**Inhomogeneity Parameter:** A parameter that indicates the deviation from adiabatic compression of a homogeneous body.

**Komatiite:** An igneous rock with ultramafic composition. The eruption of such ultramafic lavas is mainly observed in the Archean period (more than 2.5 billion years ago).

**Lithosphere:** Near-surface strong layer of the Earth (about 50–100 km thick). The (old) oceanic lithosphere is strong and moves without much deformation. The continental lithosphere is weak and is deformed when a significant force is applied.

**Magma Ocean:** A hypothetical thick layer of magmas that may have occurred on the Moon or on the Earth in their early history.

**MORB:** Mid-Oceanic Ridge Basalt. The basalt generated at the mid-ocean ridges. The oceanic crust is mainly composed of this basalt.

**OIB:** Ocean Island Basalt, which forms volcanoes in ocean islands (e.g., Hawaii). Its major-element composition is similar to MORB, but its trace-element composition is characterized by the enrichment of incompatible elements.

**Peridotite:** A ultramafic rock composed mainly of olivine and pyroxenes.

**Plate Tectonics:** A unified theory of the Earth's tectonics in which the relative motion of the near-surface layer (lithospheric plates) is responsible for major tectonic activities.

**Pyrolite:** A hypothetical primitive mantle rock proposed by A. E. Ringwood. Its composition corresponds to a mixture of basalt and peridotite. The mixing ratio is rather arbitrary but a typical one is one part basalt and three parts peridotite.

**Q:** The measure of energy dissipation.  $Q^{-1}$  represents the fraction of energy dissipated per unit cycle of deformation.

**Seismic Tomography:** Seismological technique to reveal three-dimensional fine structures of the Earth.

**Wadati-Benioff Zone:** A planar zone beneath ocean trenches where seismic activity is high. The Wadati-Benioff zone represents a subducting oceanic lithosphere.

**Xenolith:** A fragment of rock that is carried up to the surface by volcanoes. Xenoliths

provide useful information as to the temperature and chemical composition of the Earth's deep interior.

### List of Works Cited

Anderson, D. L. (1989), *Theory of the Earth*, Boston: Blackwell.

Dziewonski, A. M., Woodward, R. L. (1991), *Acoust. Imaging* **19**, 785–797.

Jeanloz, R. (1990), *Annu. Rev. Earth Planet. Sci.* **18**, 357–386.

Jeanloz, R., Morris, S. (1986), *Annu. Rev. Earth Planet. Sci.* **14**, 377–415.

Lay, T. (1989), *EOS, Trans Am. Geophys. Union* **70**, 40–59.

Montagner, J.-P., Tanimoto, T. (1990), *J. Geophys. Res.* **95**, 4797–4819.

Ringwood, A. E. (1979), *Origin of the Earth and Moon*, New York: Springer-Verlag.

van der Hilst, R., Engdahl, R., Spakman, W., Nolet, G. (1991), *Nature* **353**, 37–43.

### Further Reading

Anderson, D. L. (1989), *Theory of the Earth*, Boston: Blackwell. A unique synthesis of geophysical and geochemical observations on the Earth's structure and evolution.

Fowler, C. M. R. (1989), *The Solid Earth*, Cambridge, U.K.: Cambridge Univ. Press. An introductory account of solid earth geophysics with emphasis on geodynamics.

Jeanloz, R., and Morris, S. (1986), *Annu. Rev. Earth Planet. Sci.* **14**, 377–415. An overview of temperature profiles of the Earth's interior from experimental and theoretical viewpoints.

Peltier, W. R. (Ed.) (1989), *Mantle Convection*, New York: Gordon and Breach. A collection of review papers on the Earth's global dynamics including theoretical as well as experimental studies.

Poirier, J.-P. (1991), *Introduction to the Physics of the Earth's Interior*, Cambridge, U.K.: Cambridge Univ. Press. A succinct review of fundamental condensed matter physics to understand the internal structure of the Earth.

Shankland, T. J., Bass, J. D. (1988), *Elastic Properties and Equations of State*, Washington D.C.: American Geophysical Union. A collection of classical papers on elasticity and equation of state and the internal constitution of the Earth.

Verhoogen, J. (1980), *Energetics of the Earth*, Washington D.C.: National Academy. A brief discussion of physical processes that determine the Earth's thermal regimes.

## ELECTRIC DISCHARGES

See SPARKS, ARCS, AND OTHER ELECTRIC DISCHARGES